Available online at www.sciencedirect.com

ScienceDirect

Physics Procedia 66 (2015) 270 – 277

Physics Procedia

C 23rd Conference on Application of Accelerators in Research and Industry, CAARI 2014

Monitoring of Ion Purity in High-Energy Implant via RBS

Arthur W. Haberl[a,*], Wayne G. Skala[a], Hassaram Bakhru[a,b]

[a] Ion Beam Laboratory, University at Albany, 1400 Washington Avenue, Albany, New York 12222, United States
[b] College of Nanoscale Science and Engineering, University at Albany, 1400 Washington Avenue, Albany, New York 12203, United States

Abstract

The UAlbany Dynamitron is used for high-energy ion implantation as well as for routine materials analysis. Its ion source can be run using any one of fourteen different gases, leading to concerns of contamination during an implantation. The system has the usual well-calibrated mass-separation using a magnetic analyzer. A pre- or post-implant mass spectrum through this analyzer can give a useful understanding of unintended ions within the source beam, but it does not provide direct identification for such ions as CO or diatomic nitrogen-14 when implanting silicon-28. Since these possible components have the same momentum and charge (i.e. +1), the beamline mass separator will transmit them all. Because backscattered ions from the mass-separated beam will have only atomic scattering, this allows for element detection following the breakup of any molecular ion components. The verification system consists of a back-angle particle detector along with a movable temporary target consisting of a very thin film of gold on a carbon or silicon substrate. The backscattered spectrum can then be analyzed for the presence of unwanted elements. While this does not provide for removal of the unwanted components, it does provide for the identification and measurement of the problem. We show the physical layout, software and extra details necessary for successful use of the technique.

Selection and peer-review under responsibility of the Organizing Committee of CAARI 2014

Keywords: RBS, Backscattering, Ion Implant, Ion beam

* Corresponding author. Tel.:518-442-4480;.
E-mail address: ahaberl@albany.edu

Selection and peer-review under responsibility of the Organizing Committee of CAARI 2014
doi:10.1016/j.phpro.2015.05.034

1. Need for the method

When the ion beam source is not available for routine cleaning or leak checking, the standard protection against contamination consists of mass-spectra produced by the beamline mass-analyzer. See figure 1. Multiple components are always present, but the only ones of major concern are those that have the same mass/charge ratio as the wanted beam. These cannot be removed by any adjustment to the magnetic analyzer or to its associated slits. The user can check for spectrum signatures indicating that such contamination may be present. The most obvious of these overlay ions occurs for silicon implants, where diatomic mass-14 nitrogen will pass through mixed with the silicon ions. On inspection of the mass spectrum, if the monatomic mass-14 component is small enough, then the presence of the diatomic mass-28 ion should also be small. While this is helpful, it does not provide suitable proof that the nitrogen is, in fact negligible ($^{28}Si^{++}$ is also at that mass spectrum location). To fill this gap, an additional test can be used.

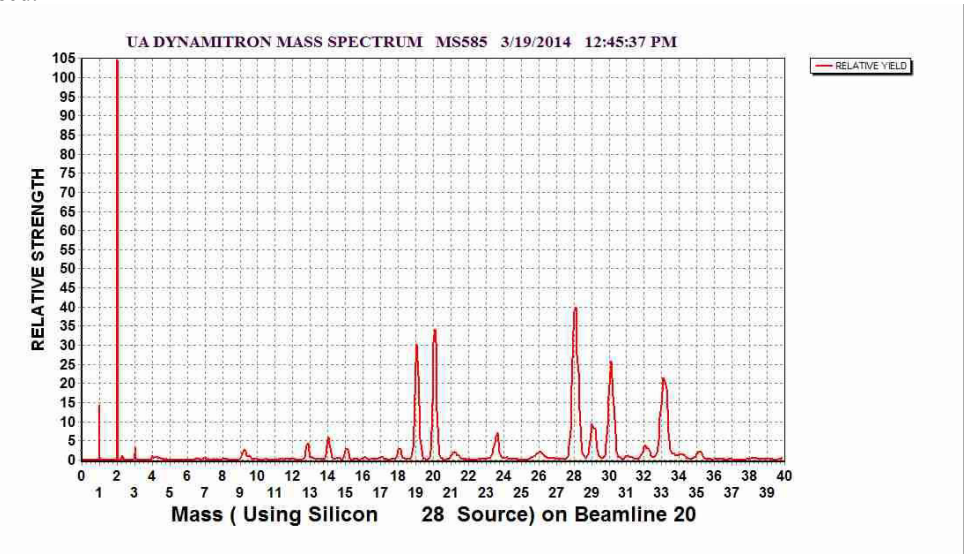

Figure 1. Mass scan showing mass 14 and mass 28 peaks as well as many rejected components.

When the beam is stopped by a solid film, any molecular components will be broken up and only atomic fragments will be available for backscattering. A standard RBS detector and electronic analyzer will then give an atomic spectrum of the beam components, thus allowing for identification of all contaminants.

2.Requirements for a reliable method.

In order to identify each element present in the beam, four items must be addressed; collision energy loss at the target face, scattering film thickness, target film substrate composition and detector response. For best element separation, the scattering foil should be thin, of high mass and mounted on a low-mass substrate. Gold is the obvious choice and carbon is the most desirable base. Gold film thickness for our work is set at 40 angstroms and is evaporated onto pyrolytic carbon. The spectrum will then consist of well-separated, near Gaussian peaks representing only the surface peak.

Analysis by standard RBS programs is not very satisfactory when applied to simultaneous beams of multiple atomic species. These programs are based on the assumption of a single value for the zero offset of the energy scale, and characterize the atomic composition of the sample rather than the atomic composition of the ion beam. Any use of backscattering for ions heavier than helium must account for a nonlinear detector response which varies for each ion mass and for each ion energy. We settled this issue by developing a new program, BEAMMASS, which is dedicated to analysis of the beam scattered from a single-component film. In its current form, it assumes

that the target is a gold film, effectively freestanding. The program does not collect the spectrum, but analyzes it after the spectral file is stored. At a later time, these functions will be fully integrated into the data acquisition computer.

3.Response of the particle detector.

In order to characterize its response, the detector action can be separated into three regions. The first region involves energy loss due to the detector dead layer, which is the electrically conductive entrance face. The second region concerns the interface between the dead layer and the active layer. This region may have a partially active-region response due to electrons excited in the dead layer which diffuse and migrate into the active layer. This intermediate region may also have a partial response due to the graded dead-layer doping profile occurring in the ion-implanted detector. The third region is the active layer where the beam is completely stopped and where dislodged electrons will be swept up in the electrical bias field and collected at the conductive faces. Within this active region, there is an energy-sensitive and mass-sensitive variation in the number of electron-hole pairs created by the stopping of the ion.

Loss of beam energy in the dead layer should be calculable using existing stopping power tables. The physical thickness of this layer is not properly known, so it was used as an adjustable parameter, settling at whatever value gave the most accurate overall results. Escape of dead layer electrons into the active region was addressed by Wall[1], but the amount of this contribution is not fully defined. This layer is therefore not addressed in the current work. The effects of the intermediate layer should be at least partly accounted for by slight adjustment of the effective dead layer thickness, thus reducing detector calculations to just two factors.

The active region response was addressed by Ratkowski[2] and others[3,4,5,6] involving various methods based on fundamentals or on 1/Z corrections. We decided to try our own method. Based on the opinions expressed by Helmut Paul and Andreas Schinner[7], the currently used method relies entirely on SRIM© data, and computes the dead layer thickness using total de/dx tables derived from SRIM[8]. We then compute the active layer response using an energy-dependent correction involving the ratio of electronic stopping power to total stopping power. This method matches experimental data very closely.

On the assumption that energy release is proportional to total stopping power but electron release is only related to the electronic stopping power, the conversion from calculated energy to apparent energy should be possible using only the SRIM dE/dX tables. We recognized that electron-hole pair creation is low at low energy and reaches a limiting value at high energy, where the stopping action is almost entirely electronic. Relative values of electron release throughout the energy range should be proportional to the ratio of electronic stopping to total stopping. This correction factor for a given ion depends on the ion energy at each point as the ion descends to zero energy, all within the active layer. The total electron release therefore cannot be determined from a single point electronic dE/dX. Since the ion will be entirely stopped within the active region, the electron release should be followed starting from the energy leaving the dead layer and continued down until the particle is stopped. To approximate this, new columns of data for the lookup tables were calculated from the SRIM stopping powers tables. Firstly, a new column, S-ratio, represents the ratio of electronic stopping power to total stopping power. For each energy interval in the stopping path, the energy loss is represented by the total stopping power, while the electron release is proportional to the S-ratio. To obtain the next table column, for each energy point in the table, the release coefficient is calculated as the average of S-ratios for all intervals below that energy point. This new C-factor, as a single correction factor, is picked by interpolation from the lookup tables and is then directly multiplied by the energy leaving the dead layer to obtain the apparent or virtual energy of the element edge.

Figure 2 illustrates the values of S-ratio (Elec/Total) and C-factor (Average) for the case of a silicon beam. Similar results are included in the lookup table for all ions from hydrogen to zinc. Figure 3 shows the dead-layer energy loss at four test energies (using total stopping power). Figure 4 shows the C-factors for the same four energies. In short, the entire response of the detector is calculated from interpolation of the lookup tables. The

virtual energy for an element edge is computed as [((E_{at} * k) – E_d) * C_{av}] where E_{at} is the energy of the arriving beam atom after breakup, k is the kinematic value for the atom on gold, E_d is the dead-layer loss computed using the energy (E_{at} * k) and C_{av} is the correction factor within the active layer, averaged from active layer energy down to zero energy. While we stopped our tables at the ion element zinc, the tables can be easily extended to include higher mass ions.

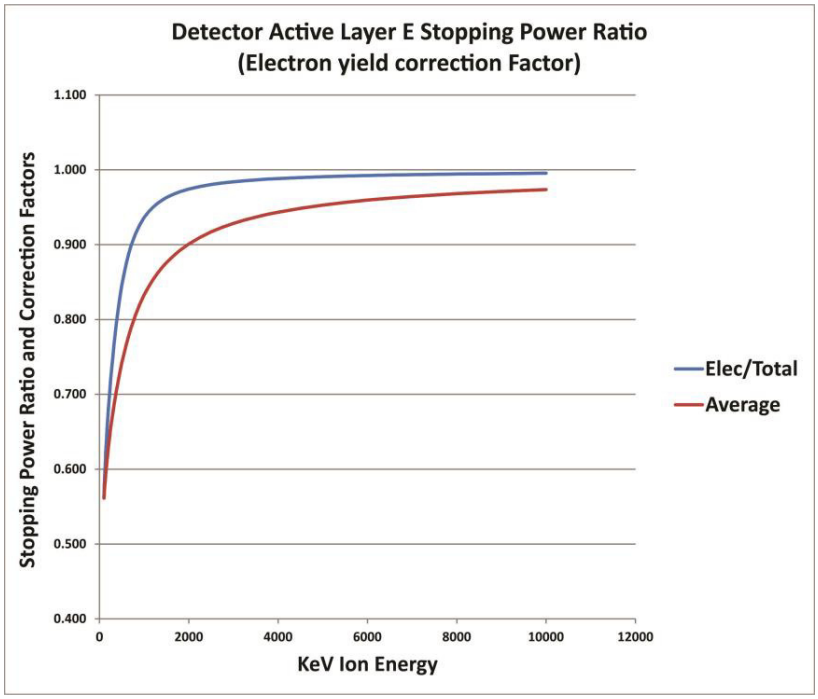

Figure 2. S-value and C factor curves for Si in Si. Similar results were computed for each ion species.

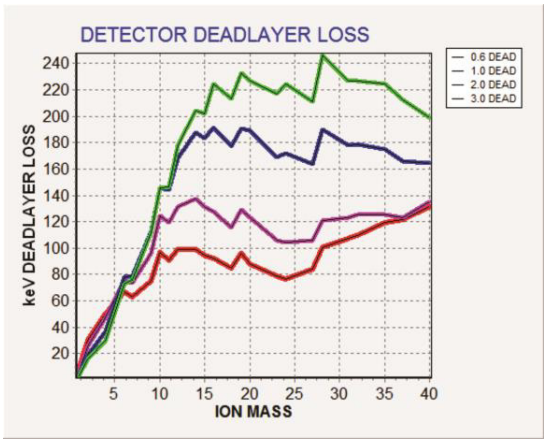

Figure 3. Deadlayer energy loss at 4 test energies.

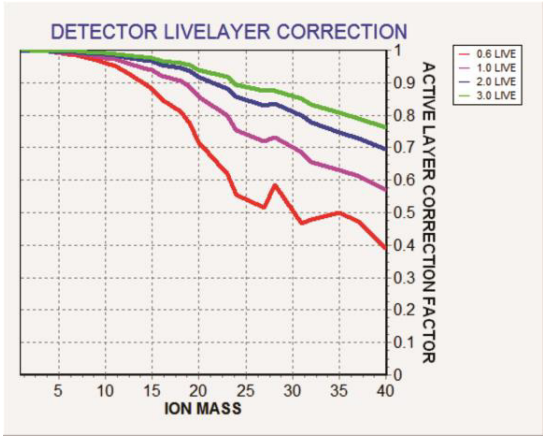

Figure 4. Active layer C-factor.

4. The Program BEAMMASS

Pulse height analysis spectra are brought in by the usual means, and the computed virtual edge simulation is plotted on top of the data spectrum. The actual form of the overlay is a Gaussian curve representing a simple estimate of the noise spread in the real spectrum.

Note that the viewable spectrum represents only the signal derived from the active layer of the detector. For each incoming ion, the actual energy represented by the left edge of the graph depends on ion species as well as ion energy. When multiple ions are displayed together, the real energy scales for each may be significantly different, and none of them are represented by the virtual energy scale that is displayed. The total spectrum therefore cannot be represented on a true energy scale. The identities of the different ions must be calculated from true energy and scaled accordingly on the virtual energy graph.

The development program can be supplied on request. The spectrum data format is a binary file unique to UAlbany, which includes all necessary parameters, including the original spectrum energy calibration as measured by helium RBS. Interested users may contact the authors for possible inclusion of reader subroutines matched to their file format.

The data-taking calibration is based on the response of a helium beam scattering from gold. The typical value for the zero offset, calculated from RUMP, is about 59 keV. Typical value for the keV/channel at UAlbany is about 2.0, but this is dependent on the amplifier settings and digitizer scales used in each laboratory. Once the data-taking scale is calibrated with a helium beam, the various ion spectra can then be read channel-by-channel by BEAMMASS, with each channel energy computed only from kev/channel. The data points are then plotted on an absolute scale whose minimum is zero and whose maximum is the ion-beam energy. This becomes a virtual energy scale, in accordance with the detector nonlinearities.

Surface-barrier detectors and implanted detectors are subject to damage by the particles they measure. To assure reasonable lifetime, the detectors need protection from high flux as well as from unnecessary exposure to beam when not in actual measurement. The pickup system should have a protective shield open only long enough to make the needed measurement, and should be additionally protected by a mechanism for automatically inserting the shield when particle rate is excessive. When used directly in the implant chamber, the active gold film should be of suitably small area so that the measurement can be made using the beam in its “ready to implant” condition. In the UAlbany system, the shallow-angle 25mm^2 detector sits about 1 meter from the target. We have considered using a

90-degree detector only about 50 cm distant, but the energy of the 90-degree scattered beam is very dependent on scattering angle, making it more difficult to use.

5. Test Applications

Since the method does analysis of ion beam components rather than implant progress, most ion beam testing can be performed on a beamline dedicated to RBS work. The normal UAlbany RBS detector in Cornell geometry is located at a scattering angle of 170 degrees, similar to the implant beamline shallow-angle detector setup. The gold film sample for calibrating this program was set at an angle of 45 degrees to the beam so that a second available detector in IBM geometry could be simultaneously used at 90 degrees scattering angle. This permits simulation of a detector to be placed in the sidewall of the implant chamber rather than in the initial hard-to-access location. Most testing of the method was performed on this RBS beamline.

All currently available beams were tested at multiple energies of 3, 2, 1 and 0.6 MeV. Lower energies were not considered due to practical limitations in the detector dead layer. While the analysis method would be very desirable for daily usage with our 400 keV ion implanter, the standard detectors now in use have thick dead layers and are not suitable for heavier ions below about 0.6 MeV. The use of detectors described by Funsten, et.al.[9] may allow extension to a somewhat lower level.

A typical response for a beam of $^{14}N^{+}$ is shown in figure 5. The peak is clear of shoulders and the remaining background shows no detectable contaminants. This contrasts sharply with the results shown in figure 6 for a $^{28}Si^{+}$ beam. The contamination with diatomic nitrogen is especially strong (nitrogen had been used shortly before this test). Cleanup progress can be monitored, as shown in figure 7. The red spectrum (N 100, Si 48) was taken first. The Orange spectrum (N 100, Si 62) was taken after short cleanup time. The green spectrum (N12, Si 100) was taken after increasing silane gas density in the ion source. In order to maintain clarity, simulations were not plotted over this graph.

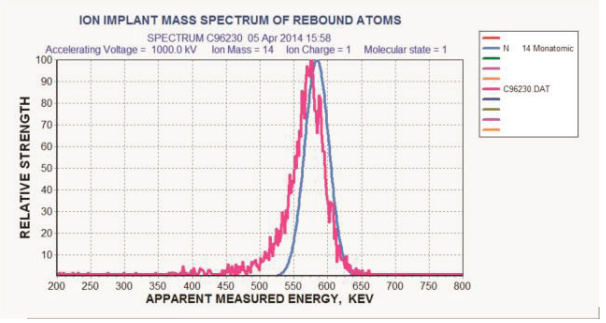

Figure 5. N-14 beam at 1 MeV.
Blue curve is the identifying simulation

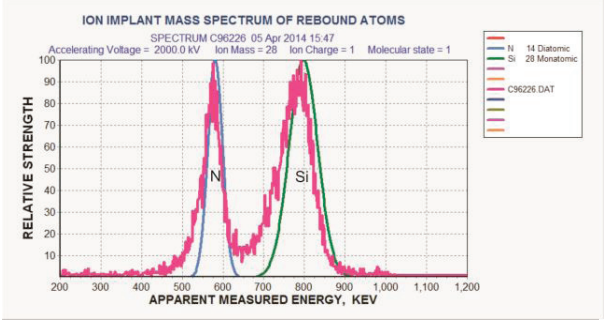

Figure 6. $^{28}Si^{+}$ beam at 2 MeV. Blue curve is sim of $^{14}N_2^{+}$(diatomic), green curve is sim of $^{28}Si^{+}$ beam.

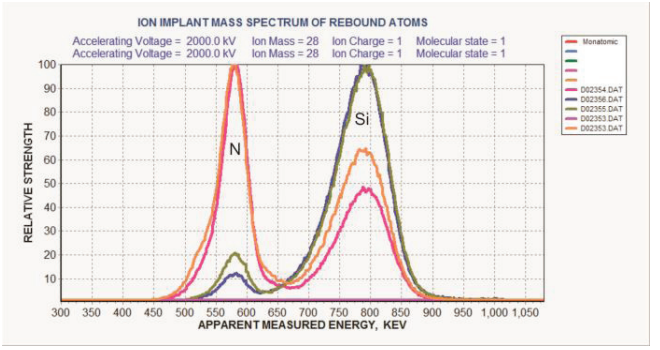

Figure 7. As in figure 5, with time sequence, but without the sim overlays.

6. Accuracy

For typical response in the method, refer to figure 8. Since the detector effective dead-layer thickness was not known by other means, an optimization routine varied this value to obtain a minimum least-squares fit to the 43 calibration points. The best dead-layer thickness value for our present line of detectors is 150 nanometers. This may or may not be the real physical value, but provided the most accurate measurements.

Overall, the fits to the experimental data are suitably acceptable, generally better than +/- 3%. See figure 9. For the set of 43 available calibration points, one sigma width is about 1.1%. There remains a small discrepancy to be explained. The dead layer for a helium beam at 2 MeV calculates at 30 keV, whereas the offset determined by RUMP is about 59 keV.

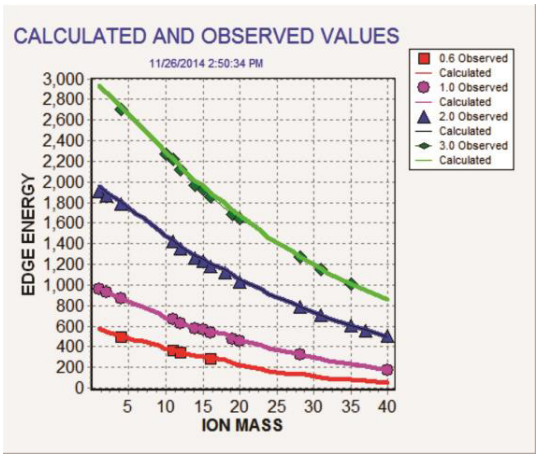

Figure 8. SIM fit for all tested points.

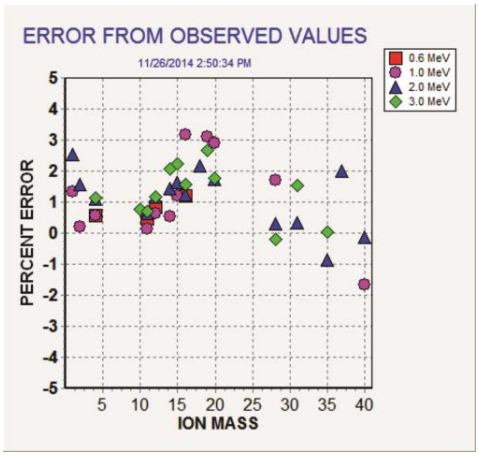

Figure 9. SIM fit errors for test data.

7. Conclusion

The method as described displays only beam components passed through the magnetic analyzer and thus should display only beam components having the same mass/charge ratio. Except for possible equal-mass isotopes of adjacent elements, all other components should be rejected by the analyser or detected by the RBS system, even including adjacent components of the mass-spectrum if the analyzer slits are left open too widely.

The detector response calculations described here may be sufficiently accurate for use in other analysis techniques using heavier ions in the region from 0.5 to 5 MeV or beyond. In the case of conventional RBS using ions heavier than helium, it should be possible to program a pre-processor which would transfer a spectrum into a linearized spectrum for direct use in existing programs (this is possible because only one ion species would be used for a given analysis).

References

[1] B. L. Wall, J. F. Amsbaugh, et al, Dead layer on silicon p-i-n diode charged-particle detectors, NIM A, Volume 744, 21 April 2014, Pages 73–79
[2] A. Ratkowski, Energy Response of Silicon surface-barrier Particle Detectors to Slow Heavy Ions, NIM 130 (1975), 533-538.
[3] L.L. Araujo, et. al, Random stopping power and energy straggling of 16O ions into amorphous Si target, Nuc. Inst. & Meth. B, 190(2002), 79-83
[4] T.D.M Weijers, et. al., Silicon detector response to heavy ions at energies of 1-2 MeV/amu, Nuc. Inst. & Meth. B, 190(2002), 387-392
[5] N.P. Barradas, et. al., Stopping power of different ions in Si measured with a bulk sample method and Bayesian inference data analysis,
[6] K. Jin, et.al., Electronic stopping powers for heavy ions in SiC and SiO2, JAP/115/4/10.1063/1.4861642
[7] Helmut Paul, Daniel Sánchez-Parcerisa, A critical overview of recent stopping power programs for positive ions in solid elements, Nuclear Instruments and Methods in Physics Research B 312 (2013) 110–117.
[8] J.F. Ziegler, SRIM, available online at SRIM.ORG.
[9] H.O. Funsten, et.al., Fundamental limits to detection of low-energy ions using silicon solid-state detectors., App. Phys. Letters, V84, #18, 3 May 2004.